CHEMISTRY
A EUROPEAN JOURNAL

Supporting Information

A Highly Practical RCM Approach towards a Molecular Building Kit of Spirocyclic Reverse Turn Mimics

Holger Bittermann, Frank Böckler, Jürgen Einsiedel and Peter Gmeiner*

Department of Medicinal Chemistry, Friedrich Alexander University Erlangen-Nürnberg, Schuhstr. 19 D-91052 Erlangen (Germany)

Contents:

2D NMR spectra of compound **12** including NOESY correlations (S2-3)

Detailed description of the theoretical investigations based on quantum chemical calculations (S4-11)

Additional references (S12)

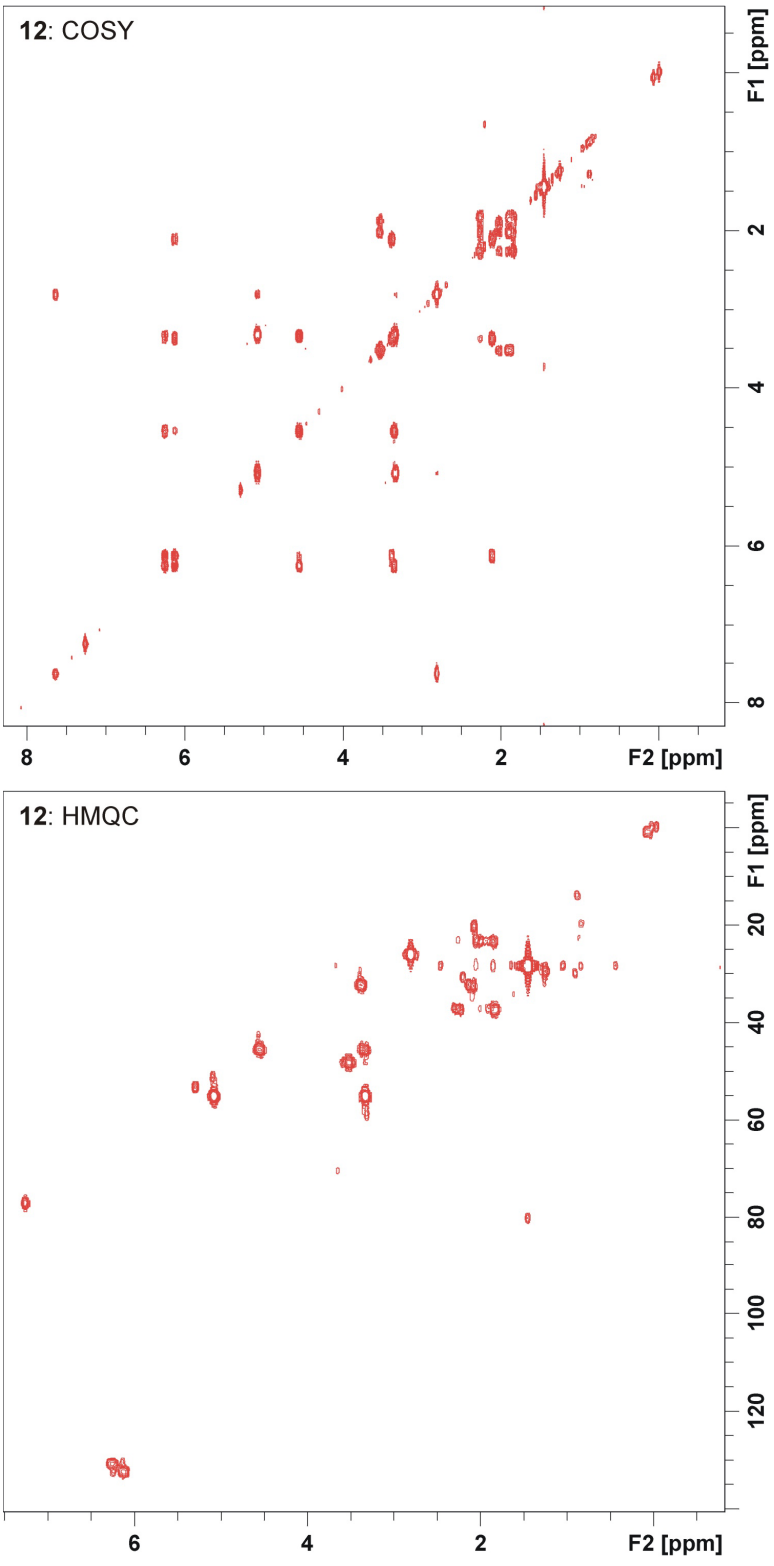

Fig. S1: COSY and HMQC spectra of **12**.

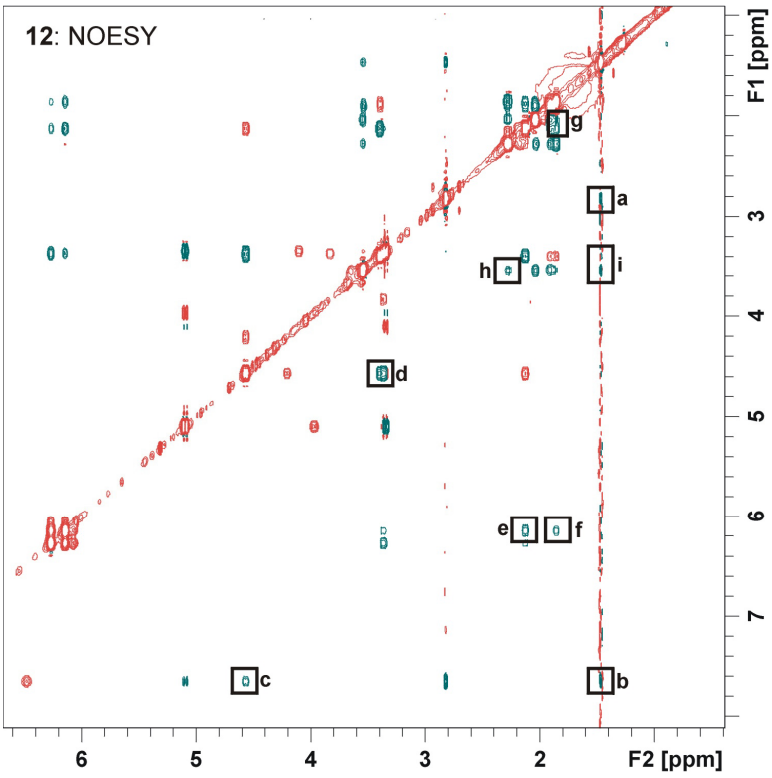

Fig. S2: NOESY spectrum of **12**.

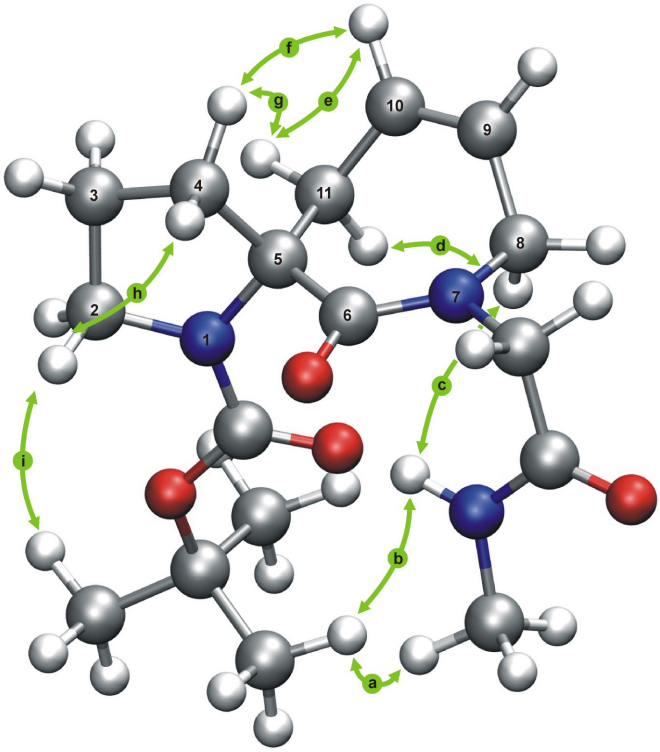

Fig. S3: Depiction of diagnostic NOESY signals in **12**.

Table S1: Final Geometries of Spiro-β-lactam, Spiro-γ-lactam and Spiro-dehydroloactams after DFT Optimizations at the B3LYP/6-311G(d,p) Level of Theory Revealing Differences in Structural Key-Parameters:

Structure	spiro-β-lactam (**3a**)	spiro-γ-lactam (**3b**)	[4.5]-spiro-dehydro-lactam (**11**)	[4.6]-spiro-dehydro-lactam (**12**)	[4.7]-spiro-dehydrolactam (**13**)	
Conformation					boat 1	boat 2
Ψ_{i+1} (N_{i+1} , C^{α}_{i+1} , C_{i+1} , N_{i+2})	124.3°	132.8°	128.5°	131.2°	147.3°	120.8°
β (C_i , C^{α}_{i+1} , C^{α}_{i+2} , N_{i+3})	11.8°	21.2°	18.1°	21.2°	32.2°	4.4°
D (O_i … H_{i+3})	2.029 Å	2.102 Å	2.025 Å	2.062 Å	2.092 Å	2.151 Å
D (O_i … N_{i+3})	3.013 Å	3.088 Å	3.019 Å	3.056 Å	3.069 Å	3.149 Å
α (C_i=O_i … H_{i+3})	150.4°	144.5°	143.7°	138.9°	139.8°	130.4°
α (O_i … H_{i+3}–N_{i+3})	162.9°	163.6°	165.5°	166.1°	161.2°	168.0°

Structure	[4.7]-spiro-dehydrolactam (**13**)		[4.8]-spiro-dehydrolactam (**14**)		
Conformation	chair 1	chair 2	conf 1		conf 2
Ψ_{i+1} (N_{i+1} , C^{α}_{i+1} , C_{i+1} , N_{i+2})	156.1°	114.2°	179.7°		113.3°
β (C_i , C^{α}_{i+1} , C^{α}_{i+2} , N_{i+3})	42.0°	-10.0°	28.5°		-8.6°
			β- turn	γ- turn	
D (O_i … H_{i+3})	2.135 Å	2.235 Å	3.478 Å	2.054 Å	2.159 Å
D (O_i … N_{i+3})	3.115 Å	3.222 Å	4.180 Å	2.918 Å	3.157 Å
α (C_i=O_i … H_{i+3})	137.9°	139.1°	104.0°	107.4°	130.7°
α (O_i … H_{i+3}–N_{i+3})	161.9°	164.8°	128.0°	141.6°	167.8°

Detailed description of the theoretical investigations based on quantum chemical calculations:

The structure of the spiro-β-lactam (**3a**) was derived from X-ray data of a suitable precursor, which was further used as a template to build the spiro-γ-lactam (**3b**) and the higher-membered rings of the spiro-dehydrolactam series (**11-14**) from. For the 7-membered spiro-dehydrolactam (**12**), available NOESY information was applied as a filter rule in an initial low level conformational sampling. Thereby, one class of conformations was easily identifiable to yield the best representation of the experimental data. For the 8-membered spiro-dehydrolactam (**13**), five discrete confomers were retrieved from initial conformational sampling and all of them were decided to be pursued to facilitate the process of structural determination. Two of these conformers had a boat-like, two a chair-like and one a twisted structure in the 8-membered ring. The twisted structure has turned out to be not a stable discrete minimum in subsequent calculations and, thus, showed a smooth transition into the boat2-conformer. Consequently, only the four persistent conformers are described in **TableS1**. In the case of the 9-membered spiro-dehydrolactam (**14**), heterogeneity of structures was anticipated from the spectroscopic data. Thus, the two predominantely occuring conformations were selected from preliminary conformational sampling to be the most plausible structures.

In summary, a total of 11 structures was submitted to a series of DFT calculations using Gaussian98[S1]. The applied optimization protocol has proven to give reasonable results in several previous studies.[S2,3] After a short semiempirial preoptimization (PM3), we used a B3LYP density functional with a 3-21G basis set in order to produce a reasonable geometry in appropriate time. Then, we increased the basis set in three subsequent steps to enhance the quality of the structure, first to the double-valence d-polarized level 6-31G(d), then to the triple-valence d-polarized level 6-311G(d), and finally to the d,p-polarized level 6-311+G(d,p) additionally adding a diffuse function.

At this level of calculation a difference of 8.5° was found between the Ψ_{i+1} angle of **3a** and **3b**, comprising that the spiro-β-lactam (**3a**) considerably approaches the Ψ_{i+1} angle (120°) of an ideal type II β-turn. Likewise, the β angle defined by Ball *et al.*[S4] as the torsion between C_i, C^{α}_{i+1}, C^{α}_{i+2}, and N_{i+3} is more tending towards the ideal value of 0° for **3a** (11.8°) than for **3b** (21.2°). Interestingly, Ψ_{i+1} and β for the [4.5]-spirodehydrolactam (**11**) is found in between those of **3a** and **3b**, with the 6-membered ring showing a Ψ_{i+1} of 128.5° and a β of 18.1°. Increasing the ring size to the [4.6]-spirodehydrolactam (**12**) yields Ψ_{i+1} and β values of 131.2° and 21.2°, respectively, which are closely appoaching the values of the five-membered ring system **3b**. For the [4.7]-spirodehydrolactam (**13**) the structural properties are strongly dependent on the conformation of the 8-membered ring. While the boat 1 and chair 1 conformations significantly increase both Ψ_{i+1} and β, the boat 2 conformation adopts an almost ideal Ψ_{i+1} of 120.8° and β of 4.4° and, thus, is second to none in the entire series. The chair 2 conformer even decreases Ψ_{i+1} and β below 120° and 0°, respectively. The conformer 1 of the [4.8]-spirodehydrolactam (**14**) adopts through its further increased ring size

very high Ψ_{i+1} and β values and can be regarded as a logical extension of the boat 1 and chair 1 conformers of **13**. However, the increased flexibility in the 9-membered ring of **14** yields with conformation 2 a totally different structure, revealing most consistency with the chair 2 conformation of **13**. While in all other structures (**3a-b,11-13**) very reasonable hydrogen-bonding parameters are found, **14** is the only one for which a minimized state (conf. 1) was identified to form more a γ- than a β-turn. This result indicates that **14** may exist in an equilibrium between a β-turn, a γ-turn and even an open state, a conclusion being also in good correspondance to the experimental findings for this compound. Conversely, this means that **14** has also a high ability to adapt to specific binding requirements when integrated in to a peptide-mimetic ligand for a particular target. For **3a, 3b, 11**-**13** and conformer 2 of **14**, the hydrogen bond distance (2.025 - 2.235 Å) between O_i and H_{i+3}, as well as the distance between O_i and N_{i+3} (3.013 - 3.222 Å), is found to be in the required range for a typical H-bond. Moreover, for these structures, also the bond angle $\alpha(O_i \ldots H_{i+3}–N_{i+3})$, which is ordinarily restricted to values > 150° for a stable hydrogen bond, is in the narrow range of 161.2-168.0° satisfying also this structural requirement.

To clarify the relevance of the calculated conformers of **13** and **14**, we subjected the optimized structures to an additional series of single point calculations modifying the density functional to B3PW91, enhancing the basis set with additional polarization functions to 6-311+G(2d,p) and 6-311+G(2df,2p), as well as treating electron correlation (alternatively to DFT) with second-order Møller-Plesset theory (MP2). Calculations on all levels are subsumed in **Table S2**. These calculations were found to give a highly consistent ranking of the conformers with almost identical relative energy differences. For the [4.7]-spiro-dehydrolactam (**13**), the boat2 conformation with its planar olefinic part folded away from the hydrogen bond (see **Figure S4**) is in general the most favoured conformer, followed by boat1 with the planar olefinic part folded towards the hydrogen bond. On all levels except for the MP2 electron correlation, the relative energy difference of boat2 versus boat1 is approximately 3 kcal/mol in favour of boat2, while this difference is reduced to 1.6 kcal/mol for MP2. This indicates that according to the Boltzmann equation, the boat1 conformation could be populated in the range of 0.5% to 7%. However, regarding the high conformational strain of this molecule, the transition state barrier between boat1 and boat2 should be considerably high. As the chair conformations are substantially more unfavourable exhibiting an energy difference to boat2 of about 7 kcal/mol (chair1) or 10 kcal/mol (chair2), we suggest that boat2 should be the predominantly found conformation (> 90%).

Table S2: Absolute energy *[hartree]* of the preferential conformer and relative energy differences *[kcal/mol]* towards the other conformers calculated at various levels of theory:

[4.7]-spiro-dehydrolactam (**13**):

method (density functional) / basis set		E_{boat2} *[hartree]*	$\Delta E_{boat1\text{-}boat2}$ *[kcal/mol]*	$\Delta E_{chair1\text{-}boat2}$ *[kcal/mol]*	$\Delta E_{chair2\text{-}boat2}$ *[kcal/mol]*
B3LYP/3-21G	Opt	-1162.195599090	+ 4.13	+ 7.35	+ 8.90
B3LYP/6-31G(d)	Opt	-1168.566735980	+ 2.96	+ 6.85	+ 9.75
B3LYP/6-311G(d)	Opt	-1168.841497600	+ 3.02	+ 6.94	+ 9.79
B3LYP/6-311+G(d,p)	Opt	-1168.897591840	+ 3.06	+ 7.03	+ 9.89
B3PW91/6-311+G(2d,p)	SP	-1168.470498260	+ 3.20	+ 7.21	+ 9.94
B3PW91/6-311+G(2df,2p)	SP	-1168.509912630	+ 3.06	+ 7.10	+ 10.06
MP2/6-311+G(2d,p)	SP	-1165.830562444	+ 1.58	+ 7.78	+ 9.73

[4.8]-spiro-dehydrolactam (**14**):

method (density functional) / basis set		E_{conf1} *[hartree]*	$\Delta E_{conf2\text{-}conf1}$ *[kcal/mol]*
B3LYP/3-21G	Opt	-1201.291566640	+ 1.17
B3LYP/6-31G(d)	Opt	-1207.874808070	+ 1.95
B3LYP/6-311G(d)	Opt	-1208.157365350	+ 2.02
B3LYP/6-311+G(d,p)	Opt	-1208.214765770	+ 1.32
B3PW91/6-311+G(2d,p)	SP	-1207.774320640	+ 1.72
B3PW91/6-311+G(2df,2p)	SP	-1207.814936270	+ 1.73
MP2/6-311+G(2d,p)	SP	-1205.028262021	+ 1.14

Figure S4: Structures **3a,b** and **11-14** optimized by DFT-calculations (B3LYP/6-311+G(d,p)):

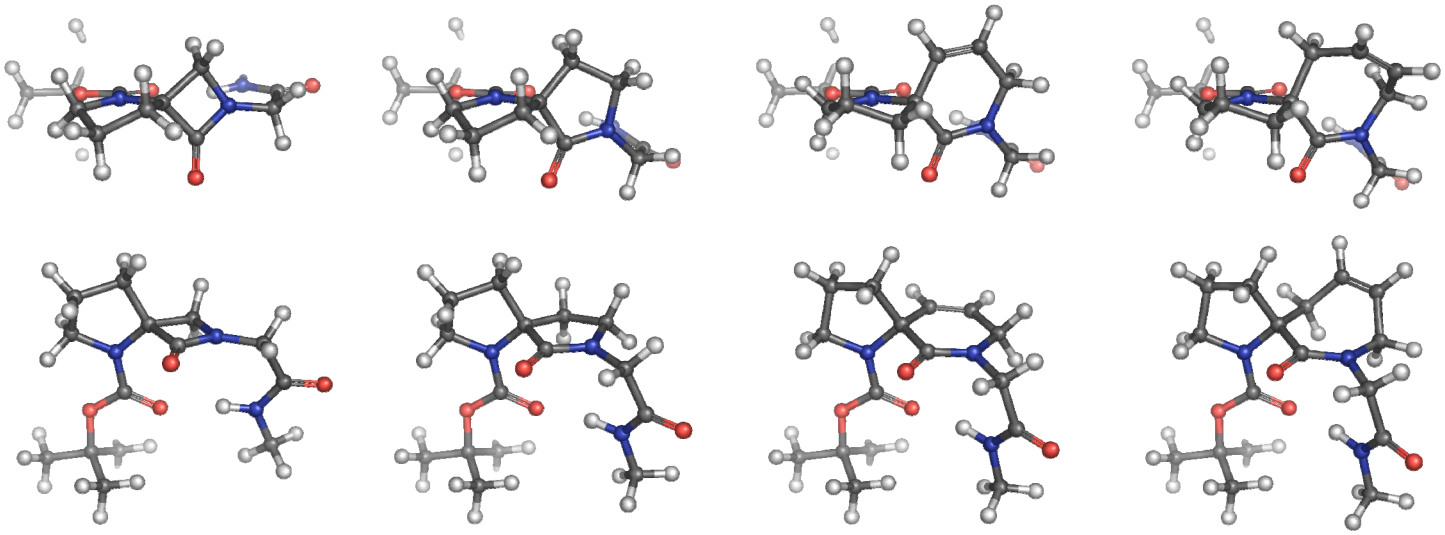

Spiro-β-lactam (**3a**) Spiro-γ-lactam (**3b**) [4.5]spiro-dehydrolactam (**11**) [4.6]spiro-dehydrolactam (**12**)

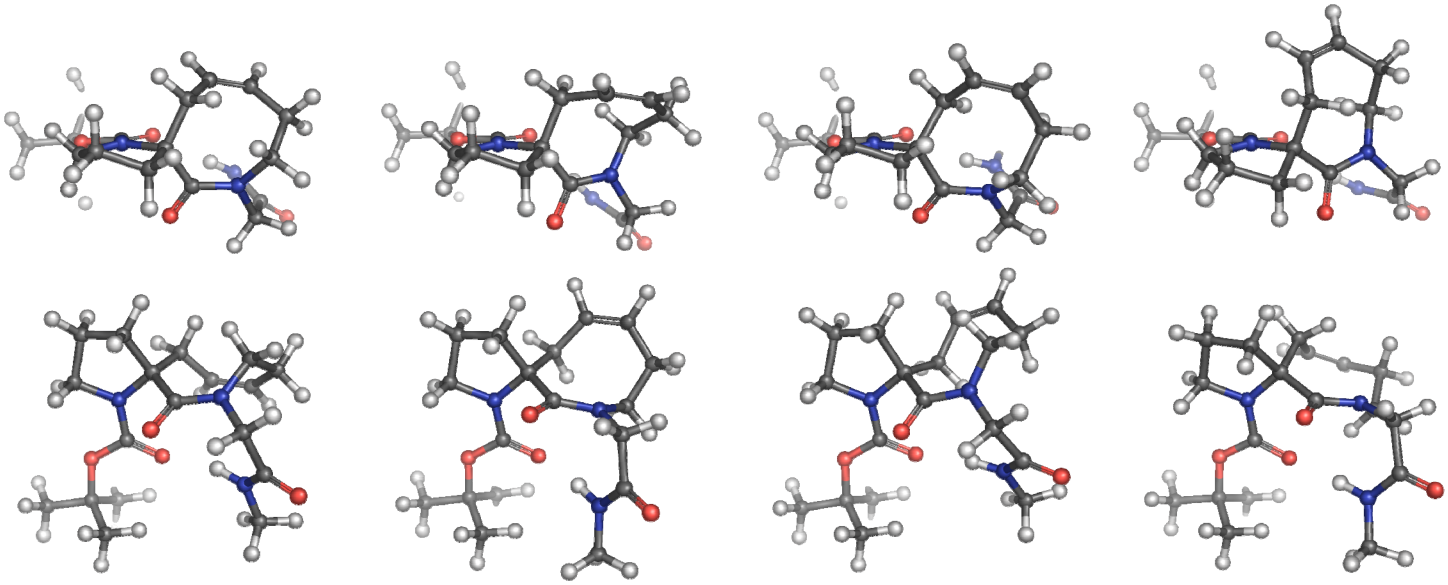

[4.7]spiro-dehydrolactam (**13**)

boat 1 boat 2 chair 1 chair 2

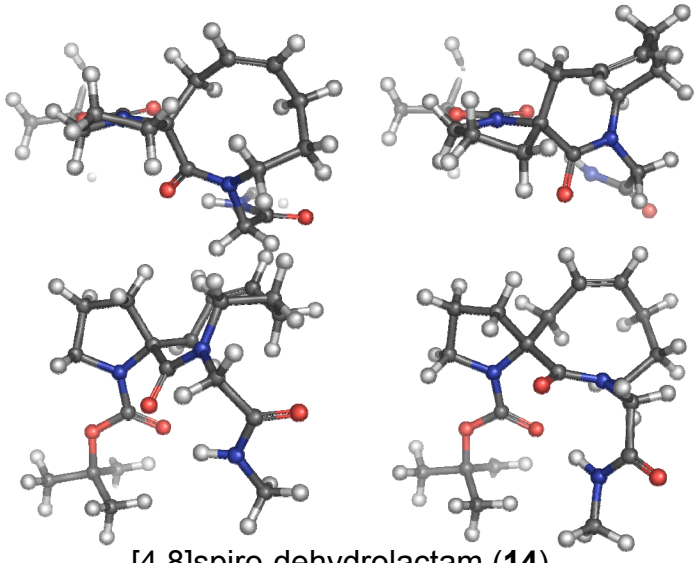

[4.8]spiro-dehydrolactam (**14**)

conformer 1 conformer 2

In order to facilitate the interpretation of our NMR-spectroscopic investigations and to corroborate the quality of the obtained structures, we have checked the conformity of their calculated magnetic shielding versus the experimental NMR data. Therefore, we calculated the magnetic shielding tensor using gauge invariant atomic orbitals[S5] (GIAO) within B3PW91 / 6-311+G(2d,p) single point calculation for all four conformations. As outlined in **Table S3+4**, considerable differences in absolute and relative chemical shifts were obtained for the four conformers. As the structural differences between boat 1, boat 2, chair 1 and chair 2 predominantly influence the hydrogens at the 8-membered ring, we have employed them as "state-specific NMR-probes" (see **Figure S5**) and, thus, calculated their chemical shifts by subtraction of the total shielding (average isotropic value) of the respective carbon atom from the total shielding of a TMS-carbon atom:

$$\delta_{x\in\{C^{\alpha}H,C^{\alpha}H',C^{8}H,C^{8}H',C^{9}H,C^{9}H',C^{10}H,C^{11}H,C^{12}H,C^{12}H'\}} = \sigma_{TMS} - \sigma_{x};$$

TMS as a reference was optimized and subjected to NMR single point calculations on the same levels as the compared structures utilizing its T_d-symmetry. In addition to these absolute chemical shift values, the relative separation ($\Delta\delta$) of the geminal hydrogen pairs (H and H') as well as of the pair of olefinic hydrogens was used as another validation criteria, which has proven to be very useful for the comparison with experimental data.[S2,3]

Figure S5

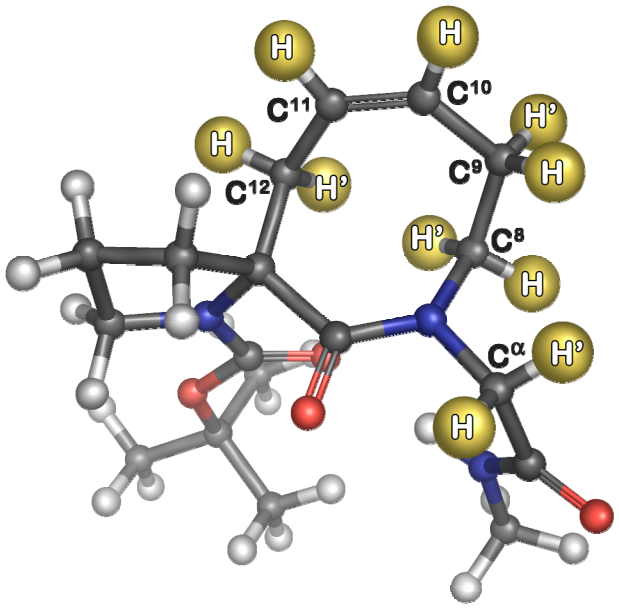

Structure of **13** in the boat 2 conformation. The hydrogen atoms used as "state-specific NMR-probes" are indicated with yellow spheres and labeled according to the numbering in **Table S3+4**.

Table S3: Comparison between experimental and calculated absolute chemical shifts δ *[ppm]* for four conformers of the [4.7]-spirodehydrolactam (**13**)

Hydrogen atoms	Exp. δ		Predicted abs. shift δ *[ppm]*				| δ_{exp} - δ_{calc} | *[ppm]*							
							298 K				220 K			
	298 K	220 K	bt 1	bt 2	ch 1	ch 2	bt 1	bt 2	ch 1	ch 2	bt 1	bt 2	ch 1	ch 2
$C^{\alpha}H$	4.62	4.65	5.51	4.76	5.53	4.31	0.89	0.14	0.91	0.31	0.86	0.11	0.88	0.34
$C^{\alpha}H'$	3.37	3.42	2.81	3.19	2.79	3.30	0.56	0.18	0.58	0.07	0.61	0.23	0.63	0.12
$C^{8}H$	3.14	3.10	2.90	2.99	3.06	3.13	0.24	0.15	0.08	0.01	0.20	0.11	0.04	0.03
$C^{8}H'$	5.03	5.16	4.28	5.17	3.31	4.36	0.75	0.14	1.72	0.67	0.88	0.01	1.85	0.80
$C^{9}H$	2.42	2.44	2.48	2.33	2.52	2.15	0.06	0.09	0.10	0.27	0.04	0.11	0.08	0.29
$C^{9}H'$	2.42	2.44	2.34	2.53	2.05	2.57	0.08	0.11	0.37	0.15	0.10	0.09	0.39	0.13
$C^{10}H$	5.55	5.60	5.71	5.78	6.62	6.47	0.16	0.23	1.07	0.92	0.11	0.18	1.02	0.87
$C^{11}H$	5.63	5.60	5.94	5.89	6.17	5.92	0.31	0.26	0.54	0.29	0.34	0.29	0.57	0.32
$C^{12}H$	2.09	2.08	2.52	1.98	2.39	2.19	0.43	0.11	0.30	0.10	0.44	0.10	0.31	0.11
$C^{12}H'$	3.42	3.45	3.01	3.57	3.87	2.66	0.41	0.15	0.45	0.76	0.44	0.12	0.42	0.79
mean							0.39	0.16	0.61	0.36	0.40	0.13	0.62	0.38

Table S4: Comparison between experimental and calculated relative chemical shift differences Δδ *[ppm]* for four conformers of the [4.7]-spirodehydrolactam (**13**)

Compared hydrogens	Exp. Δδ		Predicted abs. shift δ *[ppm]*				| δ_{exp} - δ_{calc} | *[ppm]*							
							298 K				220 K			
	298 K	220 K	bt 1	bt 2	ch 1	ch 2	bt 1	bt 2	ch 1	ch 2	bt 1	bt 2	ch 1	ch 2
$C^{\alpha}H$-$C^{\alpha}H'$	1.25	1.23	2.70	1.57	2.74	1.01	1.45	0.32	1.49	0.24	1.47	0.34	1.51	0.22
$C^{8}H$-$C^{8}H'$	1.89	2.06	1.38	2.18	0.24	1.22	0.51	0.29	1.65	0.67	0.68	0.12	1.82	0.84
$C^{9}H$-$C^{9}H'$	0.00	0.00	0.14	0.20	0.47	0.42	0.14	0.20	0.47	0.42	0.14	0.20	0.47	0.42
$C^{12}H$-$C^{12}H'$	1.33	1.37	0.48	1.59	1.48	0.47	0.85	0.26	0.15	0.86	0.89	0.22	0.11	0.90
mean							0.74	0.27	0.94	0.55	0.79	0.22	0.98	0.60

In the comparison of absolute chemical shifts (**Table S3**) the predicted values of the boat 2 conformer show clearly the best correspondance to the experimental data both determined at 298K (mean deviation: 0.16) and 220K (mean deviation: 0.13). This result becomes even more obvious, when focussing on the hydrogens attached to C^8 only, as their chemical shifts show the strongest dependence on the evaluated conformation. Only for boat 2 an almost quantitative prediction of the chemical shift for C^8H (deviation: 0.15 ppm at 298 K) and C^8H' (deviation: 0.14 ppm at 298 K) is possible. The deviations of these hydrogens even further decrease to 0.11 ppm for C^8H and 0.01 ppm for C^8H', when the NMR measuring conditions are cooled down to 220 K leading to more sharpened signals with a slight shift of δ towards a stronger separation of the signals. Thus, we conclude that at 298 K there is a slow equilibrium between the dominant boat 2 conformer and a higher energy conformer leading to movement in particular in the area of C^8, where the hydrogen signals are broadened. One putative candidate for such a higher energy local minimum could be similar to the twisted structure, which showed a transition into the boat 2 conformer during early stages of DFT-minimization. When cooling to 220 K, the signals sharpen and are even better represented by the boat 2 conformer, which is likely to be the only conformation existing at lower temperatures.
When looking at the relative separation of the chemical shifts of C^8H and C^8H', the dominance of the boat 2 versus the other conformers is clarified even more: While the experimental separation of 2.06 ppm at 220 K is almost exactly predicted by the boat 2 conformer with a deviation of 0.12 ppm, the other conformers do not even come close to this value (0.68 ppm for boat 1, 0.84 ppm for chair 2 and 1.82 ppm for chair 1).
In conclusion, based on its global minimum energy, as well as an almost ideal correspondance to experimental ^{1}H-NMR data, we suggest that boat 2 is the predominant conformer.

For the [4.8]-spiro-dehydrolactam (**14**), the low energy gap found between conformer 1 and 2, which we calculated on the same levels of theory as the conformers of **13** (**Table S2**), indicates that **14** exists in an equilibrium of at least these two conformers at room temperature. Due to our calculations, conformer 1 tends to be preferred over conformer 2 by about 1.1 to 2.0 kcal/mol, however the increase of the ring size will lower the energy barriers between these (and perhaps other) states. This corresponds to the existence of broadened signals in the experimental data, suggesting a slow exchange between different conformational states.

Additional References:

[S1] Gaussian 98 (Revision A.7), M. J. Frisch, G. W. Trucks, H. B. Schlegel, G. E. Scuseria, M. A. Robb, J. R. Cheeseman, V. G. Zakrzewski, J. A. J. Montgomery, R. E. Stratmann, J. C. Burant, S. Dapprich, J. M. Millam, A. D. Daniels, K. N. Kudin, M. C. Strain, O. Farkas, J. Tomasi, V. Barone, M. Cossi, R. Cammi, B. Mennucci, C. Pomelli, C. Adamo, S. Clifford, J. Ochterski, G. A. Petersson, P. Y. Ayala, Q. Cui, K. Morokuma, D. K. Malick, A. D. Rabuck, K. Raghavachari, J. B. Foresman, J. Cioslowski, J. V. Ortiz, A. G. Baboul, B. B. Stefanov, G. Liu, A. Liashenko, P. Piskorz, I. Komaromi, R. Gomperts, R. L. Martin, D. J. Fox, T. Keith, M. A. Al-Laham, C. Y. Peng, A. Nanayakkara, C. Gonzalez, M. Challacombe, P. M. W. Gill, B. Johnson, W. Chen, M. W. Wong, J. L. Andres, C. Gonzalez, M. Head-Gordon, E. S. Replogle, J. A. Pople, Gaussian, Inc., Pittsburgh, PA, **1998**.

[S2] C. Lenz, F. Boeckler, H. Hübner, P. Gmeiner, *Bioorg Med Chem* **2004**, *12*, 113.

[S3] C. Lenz, F. Boeckler, H. Hübner, P. Gmeiner, *Bioorg Med Chem* **2005**, *13*, 4434.

[S4] J. B. Ball, R. A. Hughes, P. F. Alewood, P. R. Andrews, *Tetrahedron* **1993**, *49*, 3467.

[S5] K. Wolinski, J. F. Hinton, P. Pulay, *Journal of the American Chemical Society* **1990**, *112*, 825